ELSEVIER

0263-8223(95)00150-6

Composite Structures **34** (1996) 291–299

0263-8223/96/$15.00

Exact elasticity solution for buckling of composite laminates

A. Chattopadhyay & H. Gu

Department of Mechanical and Aerospace Engineering, Arizona State University, Tempe, AZ 85287-6106, USA

An exact elasticity solution is presented for the buckling of a simply-supported orthotropic plate whose behavior is referred to as cylindrical bending. The general class of problems involving the geometric configuration of any number of orthotropic layers bonded together and subjected to an inplane compressive load is also analyzed by making use of the uniform prebuckling stress assumption which is equivalent to the membrane assumption used in plate theories. The closed-form expressions for the displacements and stresses are derived and the nonlinear eigenvalue equations are presented which are used to solve for critical loads. The results obtained from the exact solution are compared with the critical loads furnished by the classical laminate theory, the first order and the refined third order shear deformation theory. The solution provides a means of accurate assessment of existing two-dimensional plate theories.

NOTATION

a,b,A_j	Constants
C'_{ij}	Reduced two-dimensional stiffness coefficients
E_L,E_T	Elastic moduli of laminar in the direction parallel and transverse to the fiber, respectively
G_{LT},G_{TL}	Shear moduli of laminar in the plane, perpendicular and parallel to the fiber direction, respectively
$f(z)$	Function of z
$\mathbf{F}$	Two-dimensional deformation gradient
h	Thickness of the plate
h_i	Thickness of the ith layer
L	Longitudinal length of the plate
m	Number of layers
m_i	Characteristic roots of the ordinary differential equation
n	Number of wave in longitudinal direction
p	Imposed compressive load distribution
q	Parameter
u,w	Displacements in x and z directions, respectively
x,z	Geometric coordinate
α	Infinitesimally small parameter
ν_{LT},ν_{TL}	Poisson's ratio of laminar
$\sigma_x,\sigma_z,\tau_{xz}$	Stress components
$\underline{\Sigma}$	Two-dimensional stress tensor

Superscript

0	Prebuckling state parameters
1	Additional state parameters
(i)	Index to identify the layer

INTRODUCTION

Anisotropic plates and laminated composite plates are usually analyzed by using approximate two-dimensional (2D) theories[1–3] based on either the classical Kirchhoff–Love hypothesis of nondeformable normals and transverse shears, or the refined displacement field accounting for the effects of transverse shear deformation and normal stress. Among the characteristics of these 2D theories, which limit its generality in the description of laminate response, are the approximation of inplane displacements through the thickness, particularly for laminates in which the stiffness properties vary dramatically from layer to layer. Other important limiting factors are the presence of

boundary conditions in the plate theories which precludes the precise calculation of boundary layer effects, such as stress concentration factors and the approximation of shear deformation, implied by the hypothesis of plate theories. Finally the assumption of a state of plane stress in the constitutive relations eliminates the possibility of rigorous calculation of interlaminar stresses.

To assess the validity of these approximate theories, rigorous analytical solutions based on the exact theory of elasticity should be obtained for plate problems which is amenable to such analysis. Such benchmark elasticity solutions are valuable for laminated composite plates with inherent anisotropy in material and inherent inhomogeneity among the different layers. The anisotropy and inhomogeneity lead to considerable warping of the normal to the middle surface of the plate and cause abrupt variations of stresses at the interfaces of the laminate.

A number of elasticity solutions are available for composite plates subjected to a transverse load distribution. Pagano[4] first analyzed the cylindrical bending of simply-supported composite laminates under sinusoidal transverse loads. Later investigations include bending of finite rectangular plates,[5,6] off-axial layers,[7,8] and localized loading.[9] These elasticity solutions have enabled us to quantify the errors associated with various laminated plate theories.[10]

To address the problem of buckling of composite plates subjected to axial compression, early researches have been conducted through the application of classical laminate theory.[11] For more accurate representations of the transverse shear and the transverse normal effects, various modifications in the classical theory of laminated plate have been performed.[1–3,12,13] These higher-order plate theories can be applied to the buckling problems with the potential of improved predictions of the critical load. However, no effort has been reported in presenting a solution based on the theory of elasticity to the problem of buckling of composite plate, against which results from various plate theories could be compared.

Towards this objective, an exact elasticity solution is presented for buckling of simply supported orthotropic plates and laminated composite plates whose behavior are referred to as cylindrical bending. Numerical results are presented for a single-layer orthotropic plate, a three-layer cross-ply laminated plate and a four-layer angle-ply laminated plate under axial compressive pressure and are compared with those obtained using several different plate theories. The developed theory therefore serves as a tool to assess the accuracy of the classical plate theory and existing improved plate theories for composites with moderately thick and thick constructions.

SOLUTION FOR ORTHOTROPIC PLATES

For an elastic body in a state of plane strain with respect to the xz plane (Fig. 1), the equations of equilibrium are written in terms of the 2D stress tensor $\sum$ and the 2D deformation gradient $\mathbf{F}$ as follows.

$$\mathrm{div}(\sum \cdot \mathbf{F}^T)=0 \tag{1}$$

where the deformation gradient $\mathbf{F}$ can be expressed by the derivatives of the displacements u and w.

$$\mathbf{F}=\begin{bmatrix} 1+u_{,x} & u_{,z} \\ w_{,x} & 1+w_{,z} \end{bmatrix} \tag{2}$$

where the comma denotes partial differentiation with respect to the index that follows. The equilibrium eqn (1) can be rewritten as follows.

$$\begin{aligned} &[\sigma_x(1+u_{,x})+\tau_{xz}u_{,z}]_{,x}+[\tau_{xz}(1+u_{,x})+\sigma_z u_{,z}]_{,z}=0 \\ &[\sigma_x w_{,x}+\tau_{xz}(1+w_{,z})]_{,x}+[\tau_{xz}w_{,x}+\sigma_z(1+w_{,z})]_{,z}=0 \end{aligned} \tag{3}$$

in which, σ_x is the inplane stress along x direction, σ_z is the transverse normal stress and τ_{xz} is the transverse shear stress.

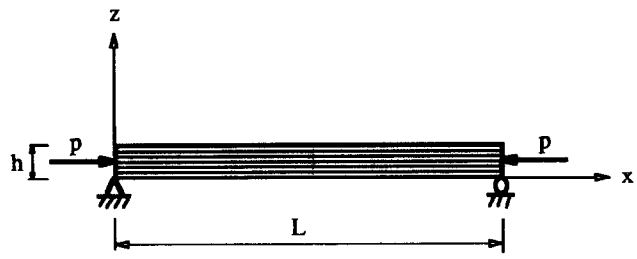

Fig. 1. Geometry of the composite plate.

At the critical load, there are two possible infinitely close positions of equilibrium. Denoting by superscript $(\,)^0$ the components of the stresses or the displacements corresponding to the primary position, a perturbed position is defined as follows.

$$\sigma_x=\sigma_x^0+\alpha\sigma_x^1,\ \sigma_z=\sigma_z^0+\alpha\sigma_z^1,\ \tau_{xz}=\tau_{xz}^0+\alpha\tau_{xz}^1$$
$$u=u^0+\alpha u^1,\ w=w^0+\alpha w^1 \tag{4}$$

where α is an infinitesimally small quantity and $\alpha(\,)^1$ are the stresses or the displacements to which the points of the body must be subject to in order to shift them from the initial position of equilibrium to the new equilibrium position. Inserting eqn (4) into eqn (3) and collecting the α terms, the buckling equations are obtained.

$$[\sigma_x(1+u_{,x}^0)+\tau_{xz}u_{,z}^0+\sigma_x^0(1+u_{,x})+\tau_{xz}^0u_{,z}]_{,x}+[\tau_{xz}(1+u_{,x}^0)+\sigma_zu_{,z}^0+\tau_{xz}^0(1+u_{,x})+\sigma_z^0u_{,z}]_{,z}=0 \tag{5}$$
$$[\sigma_xw_{,x}^0+\tau_{xz}(1+w_{,z}^0)+\sigma_x^0w_{,x}+\tau_{xz}^0(1+w_{,z})]_{,x}+[\tau_{xz}w_{,x}^0+\sigma_z(1+w_{,z}^0)+\tau_{xz}^0w_{,x}+\sigma_z^0(1+w_{,z})]_{,z}=0$$

where the superscript $(\,)^1$ is removed for the convenience of notation. The membrane primary prebuckling state of orthotropic plates whose material axes are parallel to the geometric axes can be truly simulated by

$$\sigma_x^0=-p,\quad \sigma_z^0=\tau_{xz}^0=0. \tag{6}$$

For any kind of orthotropic layer, the exact constitutive equations can be stated as follows.

$$\begin{bmatrix}\sigma_x\\ \sigma_z\\ \tau_{xz}\end{bmatrix}=\begin{bmatrix}C'_{11} & C'_{13} & 0\\ C'_{13} & C'_{33} & 0\\ 0 & 0 & C_{55}\end{bmatrix}\begin{bmatrix}\varepsilon_x\\ \varepsilon_z\\ \gamma_{xz}\end{bmatrix} \tag{7}$$

in which, the reduced stiffness coefficients C'_{ij}, $(i,j=1,3)$ can be derived from the general 3D constitutive equations in terms of C_{ij}. The displacements for prebuckling state are derived as follows.

$$u_{,x}^0=-\frac{C'_{33}}{C'_{11}C'_{33}-C'^2_{13}}p,\quad w_{,x}^0=\frac{C'_{13}}{C'_{11}C'_{33}-C'^2_{13}}p,\quad u_{,x}^0=w_{,x}^0=0. \tag{8}$$

The simplified buckling equations are stated as follows.

$$[\sigma_x(1+u_{,x}^0)-pu_{,x}]_{,x}+[\tau_{xz}(1+u_{,x}^0)]_{,z}=0$$
$$[\tau_{xz}(1+w_{,z}^0)-pw_{,x}]_{,x}+[\sigma_z(1+w_{,z}^0)]_{,z}=0 \tag{9}$$

and the simply-supported boundary conditions for the buckling state are simulated by

$$\sigma_x(0,z)=\sigma_x(L,z)=0$$
$$w(0,z)=w(L,z)=0 \tag{10}$$

where L is the length of the plate. Using eqns (6)–(8), the above buckling equation can be expressed in terms of displacements as follows.

$$\left(1-\frac{C'_{33}}{C'_{11}C'_{33}-C'^2_{13}}p\right)[C'_{11}u_{,xx}+C'_{55}u_{,zz}+(C'_{13}+C'_{55})w_{,xz}]-pu_{,xx}=0$$

$$\left(1+\frac{C'_{13}}{C'_{11}C'_{33}-C'^2_{13}}p\right)[(C'_{13}+C'_{55})u_{,xz}+C'_{55}w_{,xx}+C'_{33}w_{,zz}]-pw_{,xx}=0. \tag{11}$$

For the simply supported plate, the solution to the boundary value problem described in eqns (10) and (11) can be obtained by assuming the following solution form

$$w=f(z)\sin qx \tag{12}$$

where, $f(z)$ is the unknown function of z and the quantity q is defined as follows.

$$q=q(n)=\frac{n\pi}{L}$$

where, L is the longitudinal length of the plate and n is number of wave in longitudinal direction. By eliminating the inplane displacement variable, u, in eqn (11), we find that the functions $f(z)$ are defined by the solution to the following ordinary differential equation

$$f^{(4)}-2aq^2f''+bq^4f=0 \tag{13}$$

where

$$a=\frac{1}{2C'_{33}C'_{55}}\left(C'_{11}C'_{33}-C'^2_{13}-2C'_{13}+C'_{55}-\frac{C'_{33}p}{1-C'_{33}/(C'_{11}C'_{33}-C'^2_{13})p}-\frac{C'_{55}p}{1+C'_{13}/(C'_{11}C'_{33}-C'^2_{13})p}\right)$$

$$b=\frac{1}{C'_{33}C'_{55}}\left(C'_{11}-\frac{p}{1-(C'_{33}/C'_{11}C'_{33}-C'^2_{13})p}\right)\left(C'_{55}-\frac{p}{1+(C'_{13}/C'_{11}C'_{33}-C'^2_{13})p}\right). \tag{14}$$

The function $f(z)$ is expressed as follows.

$$f(z)=\sum_{j=1}^{4}A_j\exp(m_jz) \tag{15}$$

where, A_j are constants, provided that the m_j are all distinct. The various values m_j are given by

$$\begin{matrix}m_1\\m_2\end{matrix}=\pm q\sqrt{a+\sqrt{a^2-b}},\quad \begin{matrix}m_3\\m_4\end{matrix}=\pm q\sqrt{a-\sqrt{a^2-b}}. \tag{16}$$

The composite material properties considered here are such that $a^2-b>0$ in eqn (16). Consequently the m_j are all real and distinct and the coefficients A_j are all real. The displacement and stress components now take the following form

$$w=\sin qx\sum_{j=1}^{4}A_j\exp(m_jz)$$

$$u=\frac{1}{(C'_{13}+C'_{55})}\left\{\sum_{j=1}^{4}\left[C'_{33}m_j-\left(C'_{55}-\frac{p}{1+C'_{13}/(C'_{11}C'_{33}-C'^2_{13})p}\right)\frac{q}{m_j}\right]A_j\exp(m_jz)\right\}\cos qx$$

$$\sigma_z=\left\{\sum_{j=1}^{4}\left[C'_{33}m_j+C'_{13}\frac{\left(C'_{55}-\frac{p}{1+C'_{13}/(C'_{11}C'_{33}-C'^2_{13})p}\right)\frac{q^2}{m_j}-C'_{33}m_j}{C'_{13}+C'_{55}}\right]A_j\exp(m_jz)\right\}\sin qx \tag{17}$$

$$\tau_{xz}=C'_{55}\left\{\sum_{j=1}^{4}\left[q+\frac{C'_{33}\dfrac{m_j}{q}-\left(C'_{55}-\dfrac{p}{1+C'_{13}/(C'_{11}C'_{33}-C'^2_{13})p}\right)q}{(C'_{13}+C'_{55})}\right]A_j\exp(m_jz)\right\}\cos qx.$$

The remaining boundary conditions at the top and the bottom surfaces of the plate, for the buckling problem, are as follows

$$\sigma_z(x,0)=\sigma_z(x,h)=0,\quad \tau_{xz}(x,0)=\tau_{xz}(x,h)=0 \tag{18}$$

where h is the thickness of the plate. Applying the boundary conditions (16) to expression (17) leads to a system of a nonlinear eigenvalue problem with four simultaneous equations for eigenvalues p and eigenvectors A_j.

SOLUTION FOR COMPOSITE LAMINATES

For the laminated composite plate (Fig. 1), denoting h_i to be the thickness of the ith layer ($i=1,2,\ldots,m$, where m is the number of layers) the total plate thickness $h=\sum_{i=1}^{m} h_i$. An assumption of the uniform prebuckling stress in each layer, which is equivalent to the membrane assumption used in plate theories, is made for the composite plates. That is

$$\sigma_x^{0(i)}=-p,\quad \sigma_z^{0(i)}=\tau_{xz}^{0(i)}=0 \tag{19}$$

in which the superscription (i) is an index used to identify quantities in the ith layer. The displacements for prebuckling state expressed in eqn (8) are valid in each layer. Therefore the solution procedure for the derived boundary value problem which is described in eqns (10)–(17) is also valid within each layer. To establish continuity of traction and displacement at the interfaces between layers we must satisfy the following conditions in local coordinates.

$$\begin{aligned}
&\tau_{xz}^{(i)}(x,h_i)=\tau_{xz}^{(i+1)}(x,0)\\
&\sigma_z^{(i)}(x,h_i)=\sigma_z^{(i+1)}(x,0)\\
&u^{(i)}(x,h_i)=u^{(i+1)}(x,0)\\
&w^{(i)}(x,h_i)=w^{(i+1)}(x,0)\quad i=1,2,\ldots,m-1.
\end{aligned} \tag{20}$$

Using the above continuity equations and the remaining boundary conditions expressed in eqn (18), a set of global nonlinear eigenvalue equations of size $4m\times 4m$ are obtained for solving the critical buckling load, p, of the laminated composite plate.

RESULTS AND DISCUSSION

As an illustrative example, the critical load was determined for an orthotropic plate with various length:thickness (L/h) ratios. The material properties (typical for graphite/epoxy composites) are listed below, where L signifies the direction parallel to the fibers, T the transverse direction, and ν_{LT} is the Poisson's ratio measuring strain in the transverse direction under uniaxial normal stress in the L direction.

$$E_L=25\times 10^6\text{ psi}\quad E_T=10^6\text{ psi}$$
$$G_{LT}=0{\cdot}5\times 10^6\text{ psi}$$
$$G_{TT}=0{\cdot}2\times 10^6\text{ psi}\quad \nu_{LT}=\nu_{TT}=0{\cdot}25.$$

In this example, L corresponds to x-direction and T corresponds to y-direction as shown in Fig. 1. Figures 2 and 3 present the critical load from the exact elasticity solution, which are normalized with respect to the value obtained using the classical laminate theory (CLT), and are compared with those obtained using the classical laminate theory, the first-order[11] and the refined third-order theory,[1,11,12] for a wide range of L/h ratios. Although the four solutions merge for sufficiently thin plates, CLT exhibits a significant deviation from the other theories as shown in Figs 2 and 3. For $L/h=5$, the critical buckling load predicted by the exact elasticity solution is only about 25% of the value predicted by CLT. However, the results of the refined third-order theory show perfect agreement with those obtained using the exact elasticity solution over a large range of the length:thickness ratios, including very thick

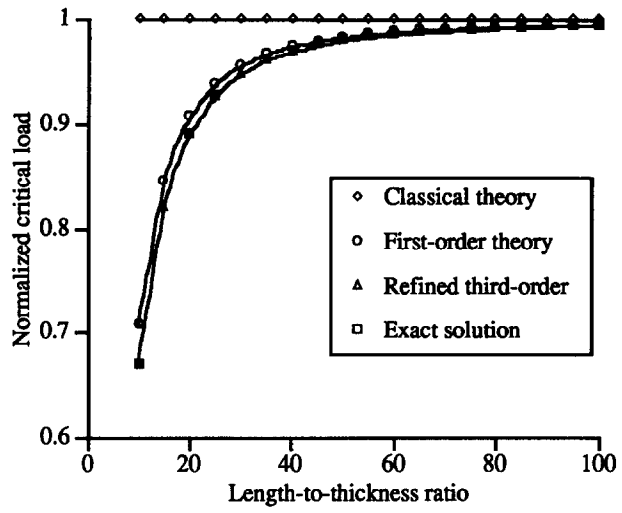

Fig. 2. Comparison of critical load for thin and moderate thick orthotropic plates.

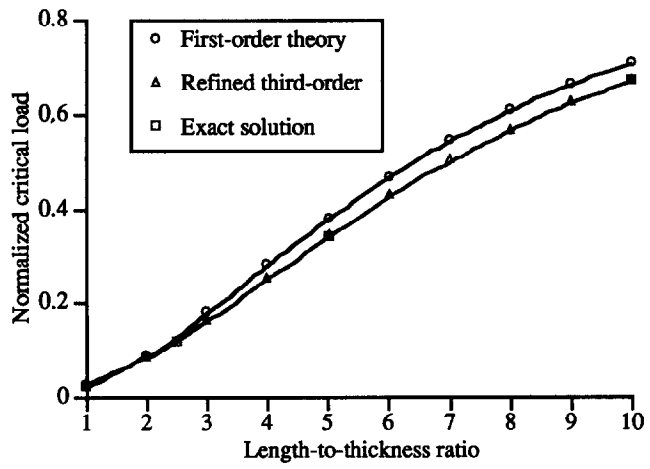

Fig. 3. Comparison of critical load for thick orthotropic plates.

plates. Since the refined third-order theory does not account for the transverse normal effect, this match indicates that the transverse normal effect is less important in the buckling problem of simply supported orthotropic plates.

Next, results are obtained for [0°/90°/0°] graphite/epoxy composite laminates and are compared with those obtained using the 2D theories described above. The results of the normalized critical load are presented in Fig. 4 for a range of length:thickness ratios varying from thin to moderately thick. In an extreme case where the plate is thin enough, all results converge to the same solution. As seen from Fig. 4, at lower values of L/h, deviations are observed from CLT. However, once again, the refined third-order theory shows good agreement with the exact elasticity solution for thin and moderately thick laminates. However, for thick laminates ($L/h<10$), Fig. 5, even the

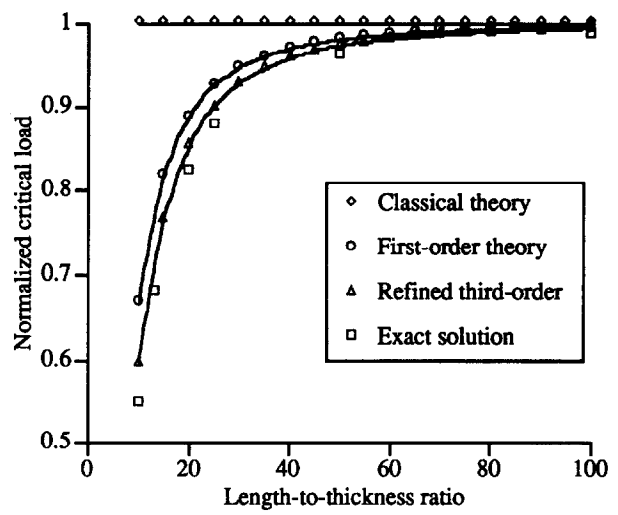

Fig. 4. Comparison of critical load for thin and moderate thick [0°/90°/0°] plates.

refined third-order theory exhibits significant deviation from the exact elasticity solution. For example, at $L/h=5$, the critical load predicted by the first-order theory is 39% higher than that predicted by the exact elasticity solution, while the critical load predicted by the refined third-order theory is 11% higher than the value obtained using the exact elasticity solution. This phenomenon is very different from what is observed for orthotropic plates and the reason is largely due to the complexity of transverse shear and normal stress distributions in composite laminates.

An angle-ply graphite/epoxy composite laminate is also examined. The stacking sequence for this example is $[-45°/45°]_S$. As shown in Figs 6 and 7, less deviations are observed in the critical load values using all four solution techniques, compared to that exhibited by the cross-ply laminates for moderately thick and thick laminates. However, the small errors exhibited by the refined third-order theory from the exact elasticity solution are observed over a wide range of L/h ratios, including very thin laminates. Although these errors are very small (not exceeding 2%), it still means that these 2D theories have some intrinsic deficiencies in modeling the buckling of angle-ply composite laminates.

Of particular interest, in the present cases, are the inplane displacement u, the out plane deflection w, and the transverse stresses τ_{xz} and σ_z at the buckling state. The elasticity solutions for these functions are illustrated in Figs 8–11 for the orthotropic plates and in Figs 12–15 for the three-layered composite laminates. For the thick orthotropic plate ($L/h=5$), it is interesting

to note that the distribution of w (Fig. 8) not only varies along the thickness but is also asymmetric with respect to the mid-plane. The distribution of τ_{xz} (Fig. 10) is symmetric to the mid-plane and the distributions of u and σ_z (Figs 9 and 11) are antisymmetric. It is expected in this case that the stress σ_z is really small due to the small value of the variation of the deflection along the thickness (less than 2% of the value of σ_z). Obviously, the distributions of u can be well fitted by the polynomials of the third order. That is why the refined third-order deformation theory can model the shear deformation of the thick plate successfully. For the

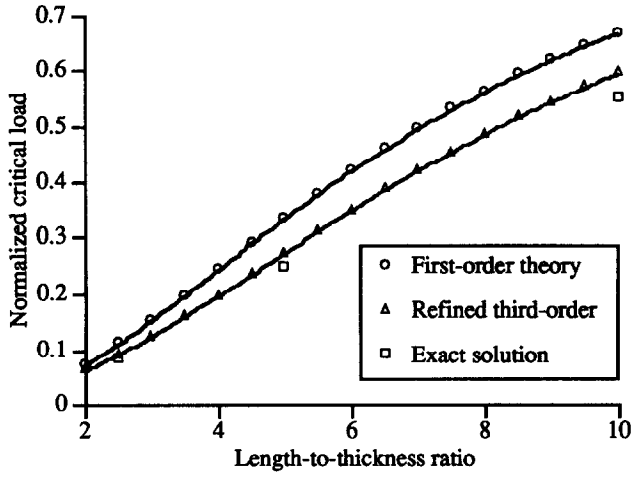

Fig. 5. Comparison of critical load for thick [0°/90°/0°] plates.

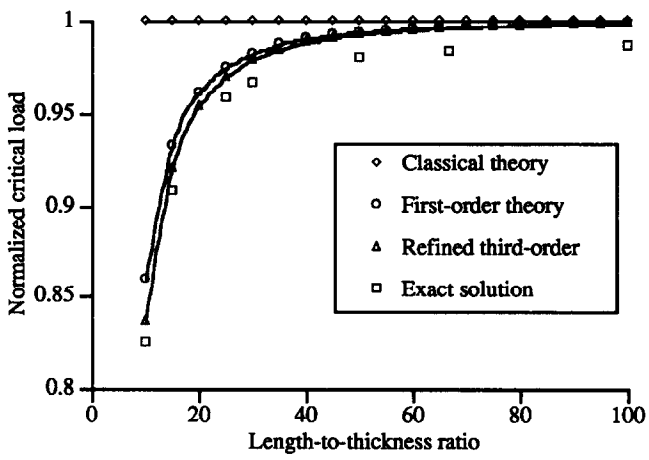

Fig. 6. Comparison of critical load for thin and moderate thick $[-45°/45°]_S$ plate.

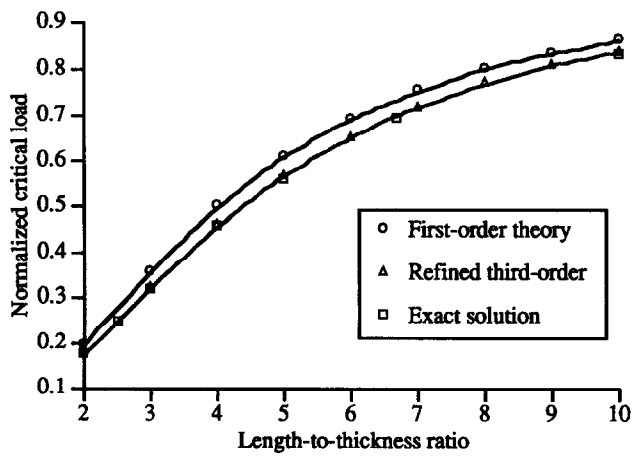

Fig. 7. Comparison of critical load for thick $[-45°/45°]_S$ plate.

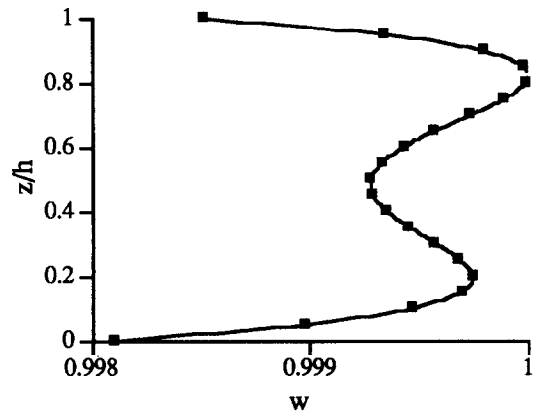

Fig. 8. Out of plane deflection distribution along the thickness for orthotropic plate, $L/h=5$.

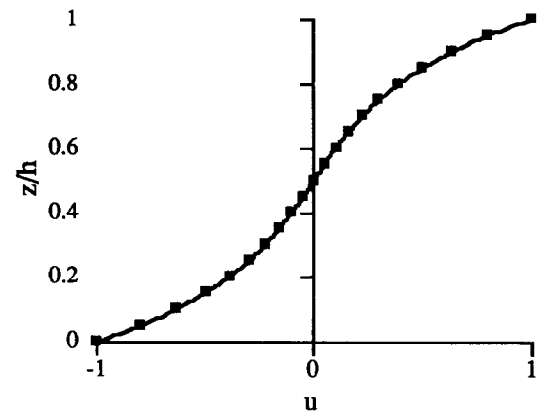

Fig. 9. Inplane displacement distribution along the thickness for orthotropic plate, $L/h=5$.

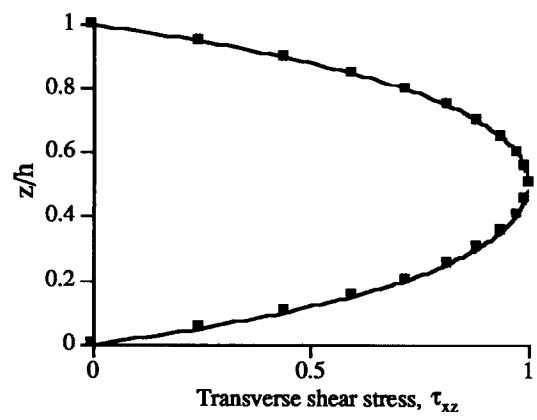

Fig. 10. Transverse shear stress distribution along the thickness for orthotropic plate, $L/h=5$.

three-layered composite laminates with moderate thickness ($L/h=15$), the curves (Figs 12–15) exhibit a very striking departure from the prediction for orthotropic plates due to the difference in geometric stiffness properties of the adjacent layers. The distribution of w (Fig. 10) is symmetric with respect to the mid-plane in this case. Since the derivatives of u and τ_{xz} are not continuous at the interfaces of layers (Figs 13 and 14), it is incorrect to use continuous polynomials to simulate the distributions of such quantities. This is why in this case the refined third-order theory is not as successful in predicting the buckling load as it is in the case of orthotropic plates. The value of σ_z is also small in this case by viewing Fig. 12.

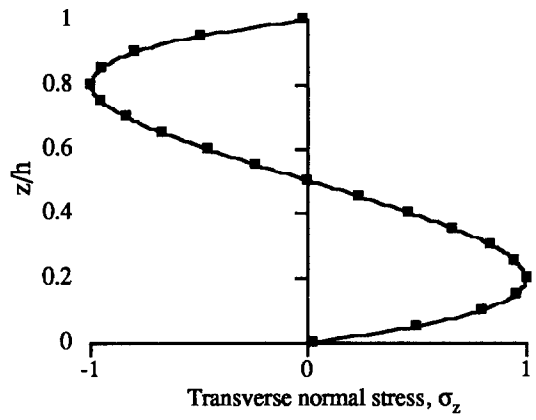

Fig. 11. Transverse normal stress distribution along the thickness for orthotropic plate, $L/h=5$.

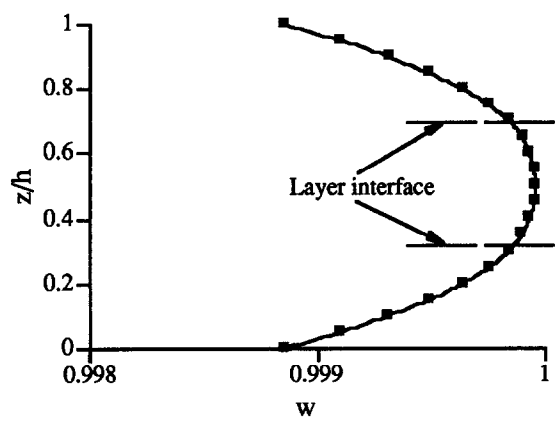

Fig. 12. Out of plane deflection distribution along the thickness for three-layered laminates, $L/h=15$.

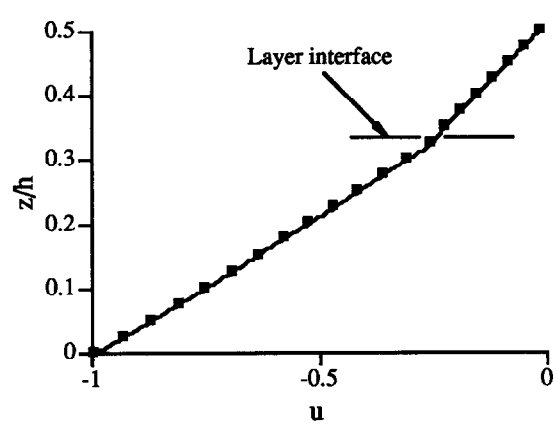

Fig. 13. Inplane displacement distribution along the thickness for three-layered laminates, $L/h=15$.

CONCLUSION

In conclusion, an exact approach to define the elasticity solution has been presented for the buckling of orthotropic plates and composite laminates consisting of arbitrary numbers of orthotropic layers whose behavior is referred to as cylindrical bending. Since the solutions are exact within the assumptions of linear elasticity, they are free from the simplifying assumptions imposed by the 2D theories. Therefore there are no distinctions between thick and thin plates and transverse shear deformation and

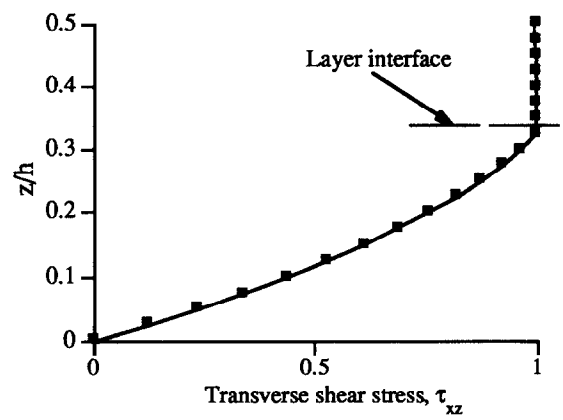

Fig. 14. Transverse shear stress distribution along the thickness for three-layered laminates, $L/h=15$.

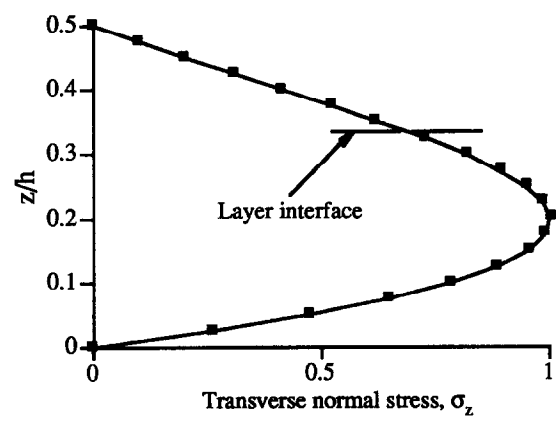

Fig. 15. Transverse normal stress distribution along the thickness for three-layered laminates, $L/h=15$.

transverse normal deformation are automatically taken into account. The following specific observations have been made.

(1) The developed theory provides a framework against which comparisons can be made of classical and other 2D theories. It also provides insight into the basic assumptions required in the formulation of more general theories for composite laminates.
(2) The solutions using the refined third-order theory for critical load converge to the exact elasticity solution with least error ($<8\%$) in all examples treated above, while solutions from CLT show an error of more than 100% for thick laminates. Based on evidence presented here, the use of the higher-order theory in the elastic design, especially for moderately thick and thin laminates, appears adequate.
(3) The higher-order theories perform more poorly in the case of multi-layer laminates compared to orthotropic plates.
(4) For angle-ply laminates, the higher-order theory produces a small but noticeable error even for very thin laminates.

ACKNOWLEDGEMENT

The research was supported by the US Army Research Office, Grant No. DAAH04-93-G-0043, Technical monitor, Dr Gary Anderson.

REFERENCES

1. Reddy, J. N., A general nonlinear third-order theory of plates with moderate thickness. *Int. J. Non-lin. Mech.*, **25** (1990) 677–86.
2. Cho, M. & Parmerter, R. R., Efficient higher order composite plate theory for general lamination configurations. *AIAA J.*, **31** (7) (1993) 1299–306.
3. Lo, K. H., Christensen, R. M. & Wu, E. M., A high-order theory of plate deformation (Part 2: laminated plates). *J. Appl. Mech.*, **44** (1977) 669–76.
4. Pagano, N. J., Exact solutions for composite laminates in cylindrical bending. *J. Composite Mater.*, **3** (1969) 398–411.
5. Pagano, N. J., Exact solutions for rectangular bidirectional composites and sandwich plates. *J. Composite Mater.*, **4** (1970) 20–35.
6. Pagano, N. J. & Hatfield, S. J., Elastic behavior of multilayered bidirectional composites. *AIAA J.*, **10** (1972) 931–3.
7. Pagano, N. J., Influence of shear coupling in cylindrical bending of anisotropic laminates. *J. Composite Mater.*, **4** (1970) 330–43.
8. Noor, A. K. & Burton, W. S., Three-dimensional solutions for antisymmetrically laminated anisotropic plates. *J. Appl. Mech.*, **57** (1990) 182–8.
9. Pagano, N. J. & Wang, A. S. D., Further study of composite laminates under cylindrical bending. *J. Composite Mater.*, **5** (1971) 521–8.
10. Noor, A. K. & Burton, W. S., Assessment of shear deformation theories for multilayered composite plates. *Appl. Mech. Rev.*, **42** (1989) 1–13.
11. Reddy, J. N., *Energy and Variational Methods in Applied Mechanics*. Wiley, New York, 1984.
12. Barbero, E. J. & Reddy, J. N., Nonlinear analysis of composite laminates using a generalized laminated plate theory. *AIAA J.*, **28** (11) (1990) 1987–94.
13. Wu, C. P. & Hsu, C. S., A new local high-order laminate theory. *Composite Structures*, **25** (1993) 439–48.
14. Thompson, J. M. T. & Hunt, G. W., *A General Theory of Elastic Stability*. Wiley, New York, 1973.